

Relaxed optimization for mode estimation in skid steering

T. M. Caldwell and T. D. Murphey

Abstract—Skid-steered vehicles, by design, must skid in order to maneuver. The skidding causes the vehicle to behave discontinuously as well as introduces complications to the observation of the vehicle’s state, both of which affect a controller’s performance. This paper addresses estimation of contact state by applying switched system optimization to estimate skidding properties of the skid-steered vehicle.

In order to treat the skid-steered vehicle as a switched system, the vehicle’s ground interaction is modeled using Coulomb friction, thereby partitioning the system dynamics into four distinct modes, one for each combination of the forward and back wheel pairs sticking or skidding. Thus, as the vehicle maneuvers, the system propagates over some mode sequence, transitioning between modes over some set of switching times. This paper presents a technique for estimating a mode sequence by optimizing a relaxation of an infinite dimensional representation of switched systems. The switching times themselves may then be estimated using switching time optimization techniques.

I. INTRODUCTION

The skid-steered vehicle (SSV) is a simple vehicle composed of a body supported by four independently driven wheels. The generalized forces applied to the vehicle’s left and right actuators dictates maneuvers. Consequently, the SSV is highly maneuverable, allowing for zero-point turns, which occur when the left wheel torques are equal but opposite to the right wheel torques and sufficiently large to overcome static friction. The high degree of maneuverability can be contrasted with the limited maneuverability of a car, which must translate in order to change orientation. The greater maneuverability comes at a price, however. The SSV’s wheels must skid laterally against the ground in order to turn and this skidding introduces uncertainties in the vehicle’s position and orientation during a maneuver due to the irregular nature of friction.

The literature on SSVs contains several approaches for dealing with these uncertainties. For instance, [5] constrains the longitudinal coordinate of the SSV’s instantaneous center of rotation, much like how a car’s instantaneous center of rotation is aligned with the rear axle. This is done in order to restrain the SSV from skidding excessively. Another approach, [18], extensively analyzes the ground characteristic by finding the shear stresses of the contact points of each wheel in order to ascertain the resistive forces with respect to different types of surfaces.

In another approach, [1] disregards the complexities of the ground interaction by modeling the SSV with a simple

unicycle model and estimating its configuration by applying well established estimation techniques. The authors fuse a dead-reckoning scheme with an inertial navigation system (INS) using a Kalman filter to estimate the configuration trajectories (position and orientation) of the SSV. The dead-reckoning scheme is designed from a kinematic model with wheel encoders (i.e. odometry) as inputs. The authors of [1] note that their approach falters when vehicle characteristics (e.g. wheel pressure, location of center of mass, ground characteristics) change slightly, requiring recalibration of the model. This sensitivity likely stems from applying a stochastic method intended for linear, or at least smooth systems, to deal with uncertainty generated from friction, a highly non-smooth dynamic system.

The authors in [1] further their work in [2] by fusing a simultaneous localization and map-building scheme (SLAM) with the dead-reckoning from above. The scheme uses a laser scan to map the vehicle’s surroundings and match with previous maps for localization. The downside of map matching is that the computational cost grows every time new objects are added. Furthermore, the authors still note that the dead-reckoning continues to falter with varying vehicle characteristics, requiring recalibration.

Consequently, due to [1], [2], we expect an intelligent estimation of skidding characteristics to improve the performance of a controller without the need for expensive hardware or computationally taxing algorithms. For instance, [22] presents an adaptive control algorithm to estimate a coefficient of their pseudo-static friction model in order to capture the SSV’s interaction with the ground while tracking a desired trajectory. Another approach, [16] apply a non-linear sliding mode observer (SMO) to estimate the SSV’s slip angle and the slip-ratios of the inner and outer wheels. The advantage of an SMO technique is that it accounts for the non-smooth period occurring when the ground contacts transition between slipping and sticking, a difficulty for continuous observers.

Similar to the reason the authors in [16] use an SMO, we treat the SSV’s wheel/ground interaction as a discrete phenomena, where the wheels discretely transition between sticking and skidding. In contrast, though, we model the SSV as a switched system and use optimization to ascertain skidding characteristics. A switched system is one that evolves over multiple distinct sub-systems by transitioning from one sub-system to another in a discrete manner [4], [6], [7], [8], [15], [19], [20], [21]. In this paper, we investigate the application of switched system optimization to estimate whether the SSV’s wheels are sticking or skidding against the ground. Primarily, we are concerned with the wheels’ skid

This material is based upon work supported by the National Science Foundation under award CCF-0907869. Any opinions, findings, and conclusions or recommendations expressed in this material are those of the author(s) and do not necessarily reflect the views of the National Science Foundation.

states in the lateral wheel direction. This is because skidding in the longitudinal direction is a force in the desired direction and can be modeled as uncertainty in the inputs.

We model the wheel-ground contact of the SSV using Coulomb friction. Coulomb friction partitions the SSV into four sub-systems for the four combinations of the front and back wheel pairs skidding or sticking against the ground. Therefore, each sub-system evolves over distinct modes of operation. The four sub-systems are: 1. all wheels sticking 2. front wheels sticking, back wheels skidding 3. front wheels skidding, back wheels sticking 4. all wheels skidding.

Thus, as the SSV drives along some path, the system propagates over some mode sequence (denoted by Ψ), transitioning between modes over some set of switching times (denoted by \mathcal{T}). Our goal is to estimate the pair (\mathcal{T}, Ψ) .

To this end, the switching times are optimally estimated using switched system optimization (see [4], [6], [7], [19], [21]). Generally, these approaches assume the mode sequence is known ahead of time. However, there has been some work on estimating mode sequences [7], [19]. In [7], the authors propose a method for removing modes that exist for short time intervals as well as a method for injecting modes for a certain time interval I depending on the sign of the gradient of that interval, $D_I J(T)$. In [19], the authors propose a method for cycling the modes a certain number of times and removing modes that exist for a short time interval between steps of a descent algorithm.

In this paper, a novel approach for estimating a mode sequence is proposed and implemented for the SSV model. The approach makes use of an infinite dimensional definition of the switched system that permits relaxation. Instead of using switching times to separate the activation periods of each mode, the infinite dimensional system uses the control inputs $u(t) = (u_1, u_2, \dots, u_N)(t)$ to specify which modes are active or inactive. If the i th mode is active, then $u_i = 1$, and if it is inactive, then $u_i = 0$. Furthermore, only one mode may be active at any given time. This definition of the system benefits from lacking a mode sequence, allowing the mode sequence to instead be estimated. However, the optimization of this definition of the system is a constrained infinite dimensional problem. Therefore, we relax the constraints that only one mode may be active and that $u(t)$ must be 1 or 0. Then, the optimal relaxed switched system can be projected back onto the set of feasible solutions in order to estimate a mode sequence. This infinite dimensional optimization may be accomplished using any optimal control technique; we use the projection operator approach presented in [9] and [10] because of its numerical stability.

One may consider the presented mode estimation approach as an infinite dimensional multiple hypothesis test where all hypotheses are compared at once by optimizing the relaxed control inputs $u(t)$. We avoid standard multiple hypothesis tests [11] because the number of hypotheses becomes quite large as the total number of modes and the expected number of switches become large (the number of hypotheses is $k = (\# \text{ of modes})^{1+(\# \text{ of switches})}$). This value, of course, assumes the maximum number of switches is

known. Furthermore, ascertaining the quality of a hypothesis depends on its associated switching times. This requires each of the k hypotheses to be optimized with respect its switching times, a difficulty for large-scale multiple testing like that in [3] and [17].

The key contribution of the paper is to show how to reformulate the SSV's hybrid dynamics as a continuous dynamical system that can be relaxed.

This paper is organized as follows: Section II introduces the SSV and decomposes its dynamics into four skid sub-systems. Section III presents a standard definition of switched systems and an infinite dimensional one. In this section, a relaxation on the infinite dimensional definition is utilized in order to estimate a mode sequence. The final section, Section IV, contains two examples applying relaxed switched system mode sequence estimation for an SSV.

II. MODELING THE SKID-STEERED VEHICLE

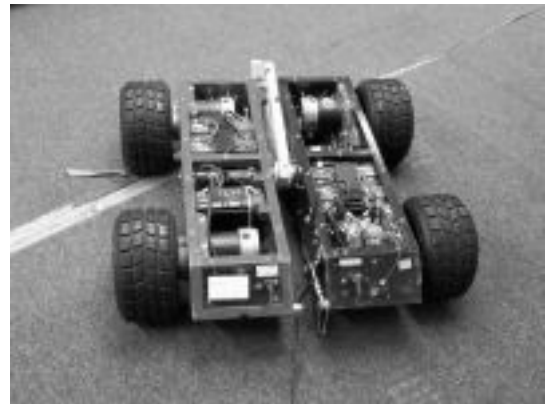


Fig. 1. The ‘‘Flexy Flyer’’.

The SSV is composed of four wheels supporting a body. The wheels are locked in alignment with the body and are independently driven. This vehicle design restricts the SSV to maneuvers dictated by differential torques to the left and right wheel pairs, resulting in lateral skidding. Therefore, in order to turn, the difference between the torques must be large enough to break the lateral static friction of the wheels against the ground. Our SSV is pictured in Fig 1.

Our representation of the SSV is the same as that in [13]. Considering the SSV as a rigid bodies, the vehicle's configuration is $x(t) = (X, Y, \theta)(t)$. The Cartesian coordinates, X and Y specify the center of geometry relative to the world frame. The orientation, θ , is the heading of the vehicle where θ increases counter-clockwise and $\theta = 0$ only occurs when the heading is aligned with the X -axis of the world frame. We disregard wheel rotations at the loss of losing the impact of the rotational inertias due to the spinning of the wheels. If the mass of the body is significantly greater than the mass of the wheels, this trade off of fidelity for computation is not a bad one. However, the wheel torques must now be transformed forces (i.e., using the $Ad(\cdot)$ operator [14]) to the center of mass of the vehicle. The inertia tensor for the

simplified model is $G = mdx \otimes dx + mdy \otimes dy + Jd\theta \otimes d\theta$, where m is the mass of the vehicle and J is the moment of inertia around the vehicle's center of mass.

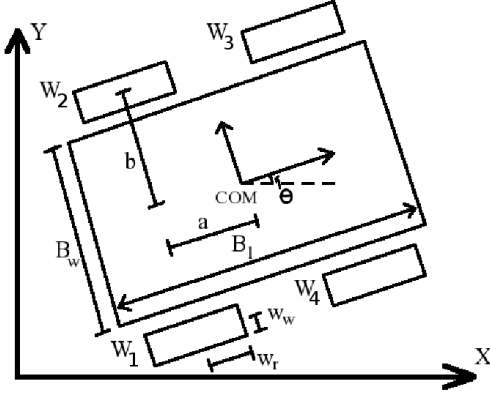


Fig. 2. Slip-steered vehicle with frame at its center of geometry.

As for the wheel/ground interaction, we use a Coulomb friction model. Coulomb friction partitions the SSV into a switched system, where switched systems are described in the next section. Assuming the geometry of the wheels as seen in Fig 2, Coulomb friction generates four distinct sub-systems that are combinations of the front and back wheels sticking or skidding with respect to the ground. Sticking is enforced using non-holonomic constraints. The four sub-systems are

	front wheels	back wheels
$\sigma = \left\{ \begin{array}{l} 1: \\ 2: \\ 3: \\ 4: \end{array} \right.$	sticking laterally	sticking laterally
	sticking laterally	skidding laterally
	skidding laterally	sticking laterally
	skidding laterally	skidding laterally

Hence, $\Sigma = \{1, 2, 3, 4\}$. The sub-systems $\sigma = 2$ and $\sigma = 3$ occur when the back or front wheels respectively are “fish tailing”. This occurs when the instantaneous center of rotation is aligned with the front wheels ($\sigma = 2$) or the back wheels ($\sigma = 3$).

The equations of motion for each $\sigma \in \Sigma$ are found using the constrained Euler-Lagrange equations (see [14]). Depending on the value of σ , the proper non-holonomic constraints are enforced. This model is similar to the way [12] generates the dynamics of a SSV with the only dissimilarity of how friction enters into the equations.

The equations of motion for $\sigma = 1$ and $\sigma = 4$ are shown. Although we also compute the equations for $\sigma = 2, 3$, we do not reproduce them here because of their algebraic

complexity.

$$f_{\sigma=1} : \begin{cases} \ddot{X} = \frac{(F_1+F_2+F_3+F_4) \cos \theta(t)}{m_B+4m_w} - c_1 \dot{X} \\ \ddot{Y} = \frac{(F_1+F_2+F_3+F_4) \sin \theta(t)}{m_B+4m_w} - c_1 \dot{Y} \\ \ddot{\theta} = 0 \end{cases}$$

$$f_{\sigma=4} : \begin{cases} \ddot{X} = \frac{(F_1+F_2+F_3+F_4) \cos \theta(t)}{m_B+4m_w} - c_4 \dot{X} \\ \quad + g\mu_K \sin \theta(t) [-\sin \theta(t) \dot{X}(t) + \cos \theta(t) \dot{Y}(t)] \\ \ddot{Y} = \frac{(F_1+F_2+F_3+F_4) \sin \theta(t)}{m_B+4m_w} - c_4 \dot{Y} \\ \quad - g\mu_K \cos \theta(t) [-\sin \theta(t) \dot{X}(t) + \cos \theta(t) \dot{Y}(t)] \\ \ddot{\theta} = \frac{12b(F_1-F_2-F_3+F_4)+12a^2g(m_B+4m_w)\mu_K\dot{\theta}(t)}{4m_w(12a^2+12b^2+w_w^2+3w_r^2)+m_B(B_l^2+B_w^2)} \end{cases} \quad (1)$$

where m_B is the mass of the body, m_w is the mass of a wheel, g is gravity, μ_K is the coefficient of kinetic friction, F_1 , F_2 , F_3 , and F_4 are the respective transformed wheel torques, and c_1 and c_4 are the respective damping coefficients.

One may be concerned with μ_K showing in the equations of motion for when $\sigma = 4$ (and $\sigma = 2, 3$). The coefficient of kinetic friction designates the loss of energy during a turn due to lateral friction. Therefore, μ_K may be a general estimation of the wheel-ground friction. Section IV provides evidence that our approach performs well with disturbances to μ_K . Nevertheless, we plan to include online estimation of this parameter in future work.

Modeling the SSV as we have in this section alleviates the necessity for some complicated model of the stick/skid transitions, which would require extensive knowledge of the ground characteristics. Instead, with our model, the estimation of these transitions is based solely on an optimization over the full configuration of the vehicle. The next section provides a method to compute such an optimization.

III. THE SWITCHED SYSTEM AND MODE SEQUENCE ESTIMATION

A switched system is defined by how the system's modes of operation evolve over time. We present two equivalent definitions of the state trajectories, $x(t) : \mathbb{R} \mapsto \mathbb{R}^n$.

A. Two Definitions of the Switched System

The first is the standard definition [4], [6], [7], [15], [19], [21]:

$$\dot{x}(t) = f(x(t), \mathcal{T}, \Psi, t)$$

$$= \begin{cases} f_i(x(t), t), & \text{where } T_{i-1} \leq t < T_i \\ \text{for } i = 1, \dots, N \end{cases} \quad (2)$$

subject to: $x(T_0) = x_0$

where N is the number of modes in the mode sequence Ψ , $\mathcal{T} = \{T_1, T_2, \dots, T_{N-1}\} \in \mathbb{R}^{N-1}$ is a monotonically increasing set of switching times, T_0 is the initial time, T_N is the final time, x_0 is the initial state, and $f_i : \mathbb{R}^n \times \mathbb{R} \mapsto \mathbb{R}^n$ is the i th mode of operation in the sequence Ψ . This definition assumes Ψ is known and therefore, optimizing a switched system utilizing this definition may only be over the switching times. For many systems, the mode sequence is not clear. We present an alternate definition which lacks a mode sequence.

The second definition uses the constrained infinite dimensional control input $u(t) : \mathbb{R} \mapsto \mathbb{R}^{\hat{N}}$ in order to specify which modes are active or inactive. If the i th mode is active, then $u_i = 1$, and if it is inactive, then $u_i = 0$. The second definition of the switched system is:

$$\begin{aligned} \dot{x}(t) &= f(x(t), u(t), t) \\ &= u_1(t)f_{\sigma=1}(x(t), t) + u_2(t)f_{\sigma=2}(x(t), t) \\ &\quad + \dots + u_{\hat{N}}(t)f_{\sigma=\hat{N}}(x(t), t) \end{aligned} \quad (3)$$

subject to: $x(T_0) = x_0$

where \hat{N} is the size of Σ and the control inputs, $u(t)$, are constrained as follows:

$$\begin{aligned} 1) \quad & \sum_{i=1}^{\hat{N}} u_i(t) = 1 \\ 2) \quad & u_1(t), u_2(t), \dots, u_{\hat{N}}(t) \in \{0, 1\} \end{aligned} \quad (4)$$

The second definition lacks a mode sequence, an assumed parameter of the first definition. Therefore, the mode sequence can instead be determined as part of an optimization.

B. Mode Sequence Estimation

Switching time optimization generally assumes a mode sequence is known [4], [6], [7], [19], [21]. This section removes the assumption by presenting a technique to estimate a mode sequence. In contrast to the two techniques mentioned in the introduction with this purpose [7], [19], our approach establishes the mode sequence based on information of the system instead of creating the sequence in an ad hoc manner and adjusting it based on its switching time optimization performance.

We recall the second definition of the switched system, Eq (3), and the constraints on the control inputs $u(t)$, Eq (4). The first constraint on u is satisfied by setting one of the inputs to be one minus the summation of all other inputs:

$$u_{\hat{N}}(t) = 1 - \sum_{i=1}^{\hat{N}-1} u_i(t).$$

As for the second constraint, let us remove it. This is the relaxation. Now, instead of modes being active or inactive, all modes are now active to some degree where the extent of activity is specified by $u(\cdot)$. Let us designate this constraint relaxation with $\hat{u}(t)$. Then, the relaxed switched system is specified by the evolution of the relaxed state trajectory, $\hat{x}(t) : \mathbb{R} \mapsto \mathbb{R}^n$:

$$\begin{aligned} \dot{\hat{x}}(t) &= \hat{f}(\hat{x}(t), \hat{u}(t), t) \\ &= \hat{u}_1(t)f_{\sigma=1}(\hat{x}(t), t) + \dots + \hat{u}_{\hat{N}-1}(t)f_{\sigma=\hat{N}-1}(\hat{x}(t), t) \\ &\quad + \left(1 - \sum_{i=1}^{\hat{N}-1} \hat{u}_i(t)\right)f_{\sigma=\hat{N}}(\hat{x}(t), t) \end{aligned}$$

subject to: $\hat{x}(T_0) = x_0$. (5)

The optimization of the relaxed switched system is over $\hat{u}(t)$:

$$\arg \min_{\hat{u}} J(\hat{u}).$$

where $J(\hat{u})$ is

$$J(\hat{u}) = \int_{T_0}^{T_N} \ell(\hat{x}(\tau), h(\tau)) d\tau + m(\hat{x}(T_N), h(T_N)). \quad (6)$$

Minimizing $J(\hat{u})$ over \hat{u} is an infinite dimensional optimization problem constrained to Eq (5). The optimization can be accomplished with the trajectory functional optimization approach using a projection operator, shown in [9]. Alternatively, any other optimal control technique may be employed.

Once the optimal \hat{u}^* is found, a mode sequence may be generated by projecting the corresponding optimal system onto the set of feasible solutions. At any given time, the projection sets the most active mode (i.e. the one corresponding to the greatest \hat{u}) as the single active mode and sets the rest as inactive, thereby satisfying the constraints on u once more. The estimated mode sequence, Ψ , is thus the sequence of most active modes. Also, the collection of times for which the most active modes transition may be used as the initial switching times, \mathcal{T}_θ . The pair $(\mathcal{T}_\theta, \Psi)$ are initial parameters for switching time optimization.

IV. EXAMPLES

We present two examples simulated in Mathematica. For all examples, the SSV has dimensions $a = 0.16\text{m}$, $b = 0.28\text{m}$, $B_l = 0.8\text{m}$, and $B_w = 0.6\text{m}$, and masses $m_B = 70\text{kg}$ and $m_w = 2.5\text{kg}$ (refer to Fig 1 and Eq (1)). The coefficient of kinetic friction is assumed to have a mean of 0.8, so μ_K is set to 0.8.

The first example estimates a mode sequence using the technique described in Section III-B. The measured configuration trajectories are simulated assuming a perfect model of the SSV and perfect sensors.

The second example demonstrates how our mode estimation performs in the presence of sensor and model disturbances. Moreover, this example demonstrates that the results from the mode estimation can be used in conjunction with switching time optimization to good affect. See [4], [6], [7], [21] for switching time optimization algorithms.

A. Example 1

The SSV is driven with the wheel torques shown in Fig 3 and initial state $x(0) = 0$. Initially, none of the wheels are skidding laterally (i.e. initially $\sigma = 1$). At some time shortly after $t = 5\text{s}$, the difference in torques becomes large enough to break the lateral static friction holding it in sub-system $\sigma = 1$ and the vehicle begins to turn left. During the turn, it is not clear which sub-system the SSV switches into, but let us assume the vehicle switches into the all wheels skidding laterally sub-system, $\sigma = 4$. At some time after $t = 10.5\text{s}$, the vehicle returns to $\sigma = 1$ due to the 0 torque difference no longer injecting energy into the wheel's lateral direction and because of the energy dissipation from skidding. Therefore, let us assume for this example that the desired mode sequence is $\Psi^d = (1, 4, 1)$, where the system transitions over desired switching times $\mathcal{T}^d = (5, 11)^T$.

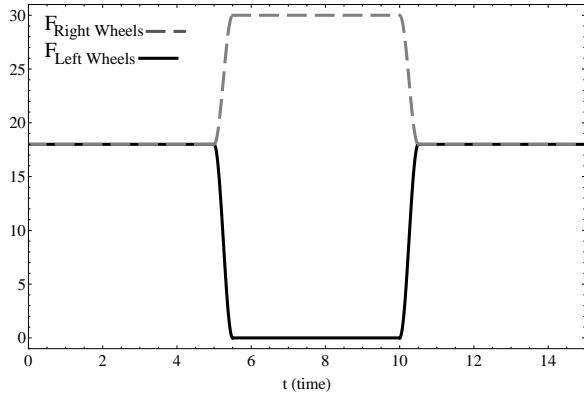


Fig. 3. The applied torques to the left and right wheels over the time interval.

Normally, the measured trajectories, $h(t)$, are measured from data collected by sensors such as a GPS. For now, we simulate $h(t)$, but in future work we will test the mode estimation on the SSV pictured in Fig 1 using sensors. For this example, we assume our SSV model is perfect. We simulate $h(t)$ with the desired mode sequence, $\Psi^d = (1, 4, 1)$, and the desired switching times $\mathcal{T}^d = (5, 11)^T$. Accordingly, the goal for this example is to estimate the mode sequence by finding the optimal control inputs of the relaxed switched system and projecting this relaxed solution onto the set of feasible solutions, as described in Section III-B.

For the cost function, we use a quadratic performance index. Therefore, Eq (6) has $\ell(\cdot, \cdot)$ and $m(\cdot, \cdot)$ equal to

$$\begin{aligned} \ell(\hat{x}(\tau), h(\tau)) &= \frac{1}{2} (\hat{x}(\tau) - h(\tau))^T Q (\hat{x}(\tau) - h(\tau)) \\ &+ \frac{1}{2} (\hat{u}(\tau) - \hat{u}_d(\tau))^T R (\hat{u}(\tau) - \hat{u}_d(\tau)) \end{aligned}$$

and

$$\begin{aligned} m(\hat{x}(T_N), h(T_N)) &= \frac{1}{2} (\hat{x}(T_N) - h(T_N))^T P \\ &\cdot (\hat{x}(T_N) - h(T_N)) \end{aligned}$$

where Q and P are symmetric semi-positive definite (i.e. $Q^T = Q \geq 0$, $P^T = P \geq 0$), R is symmetric positive definite (i.e. $R^T = R > 0$), u_d are the desired control inputs and $\hat{x}(t)$ is the relaxed state trajectory, which is the solution to

$$\begin{aligned} \dot{\hat{x}}(t) &= \hat{f}(\hat{x}(t), \hat{u}(t), t) \\ &= \hat{u}_1(t) f_{\sigma=1}(\hat{x}(t), t) + \hat{u}_2(t) f_{\sigma=2}(\hat{x}(t), t) \\ &+ \hat{u}_3(t) f_{\sigma=3}(\hat{x}(t), t) + \left(1 - \sum_{i=1}^3 \hat{u}_i(t)\right) f_{\sigma=4}(\hat{x}(t), t) \end{aligned}$$

subject to: $\hat{x}(T_0) = x_0$.

We choose \hat{u}_d to be $\hat{u}_d = (1, 0, 0)^T$. This choice places preference on the most active sub-system being $\sigma = 1$. We did this because $\sigma = 1$ is the only sub-system that can exist without losing energy from skidding. All other sub-systems

will eventually decay to $\sigma = 1$ if the vehicle is driven with zero wheel torque difference.

Letting the state vector be $x(t) = (\dot{X}, X, \dot{Y}, Y, \dot{\theta}, \theta)^T(t)$, we choose $Q = \text{diag}(70, 70, 70, 70, 70, 70)$, $R = \text{diag}(1, 1, 1)$ and compute P such that it is approximately compatible with Q and R .

The cost function is minimized using the trajectory functional optimization approach shown in [9]. This results in the optimal control inputs shown in Fig 4. Clearly, \hat{u}_1 specifies that $\sigma = 1$ is the most active mode initially. At $t = 4.9871$ s, $\sigma = 4$ becomes the most active mode and at $t = 10.9975$ s, $\sigma = 1$ returns to being the most active. Therefore, the estimated mode sequence is $\Psi = (1, 4, 1)$ with switching times $\mathcal{T} = (4.9871, 10.9975)^T$. The estimated Ψ is the desired mode sequence, Ψ^d , and the estimated switching times closely approximate $\mathcal{T}^d = (5, 11)^T$.

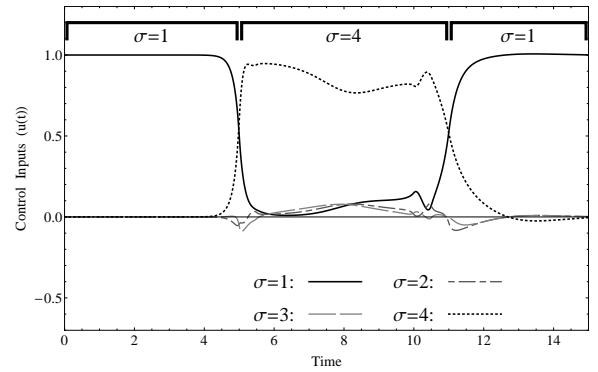


Fig. 4. The optimal relaxed control inputs for Example 1. Each control input corresponds to a sub-system σ . The sequence of greatest control inputs corresponds to a mode sequence of $\Psi = (1, 4, 1)$. These modes transition at times $\mathcal{T} = (4.9871, 10.9975)^T$

B. Example 2

In contrast to Example 1, Example 2 includes model and sensor disturbances, but otherwise, it uses the same system, wheel torques, $\Psi^d = (1, 4, 1)$ and $\mathcal{T}^d = (5, 11)^T$. The following is how we generate the perturbed measured trajectories, denoted $\bar{h}(t)$, due to model and sensor disturbances.

First, we assume the ground contains imperfections (egs: the ground is wet, it is deteriorated). Therefore, the coefficient of friction, μ_K , is not constant. The imperfections are modeled as a random walk entering additively to the coefficient of friction. This alters $\dot{x} = f_{\sigma=i}$ for $i = 2, 3, 4$ such that μ_K becomes $\mu_K \leftarrow \mu_K + \chi$ where χ is a pseudo-Gaussian signal with a mean of 0 and a standard deviation of 0.5, but where χ differs from a pure Gaussian signal in that $\mu_K + \chi$ is not allowed to be less than 0. This disturbance results in measured configuration trajectories $\bar{h}_1(t)$.

Second, let us suppose we have a lone GPS sensor which, of course, imperfectly senses the configuration of the vehicle. The GPS we will use on the SSV in Fig 1 is Garmin's GPS 16x HVS. It has a positional accuracy of < 3 meters when WAAS is enabled, a velocity accuracy of < 0.1 knots rms (i.e. < 0.0514 m/s rms) and a sample rate of 1Hz. The

sample rate restricts us to 16 data points. Since the positional accuracy is the absolute position from the latitude/longitude coordinate (0,0), and we only need the (X, Y) offset from the initial reading, the accuracy of (X, Y) should be better than < 3 meters. Instead of “guessing” what this accuracy is and basing the disturbance model from that, we instead base the disturbance from the velocity accuracy and integrate to find the positional disturbance.

The velocity components, $(\dot{X}, \dot{Y})(t)$, of $\bar{h}_1(t)$ are sampled at 1Hz. Each sample is perturbed with a random magnitude generated from a uniform distribution of numbers from the interval $(-0.051\bar{4}, 0.051\bar{4})$ and a uniformly distributed random angle. The samples are interpolated with splines and integrated to find $(X, Y)(t)$. The orientation and turning velocity is numerically calculated from $(X, Y)(t)$, fulfilling the composition of $\bar{h}(t)$. Figure 5 compares the perturbed measured trajectories $\bar{h}(t)$ with the unperturbed measured trajectories $h(t)$.

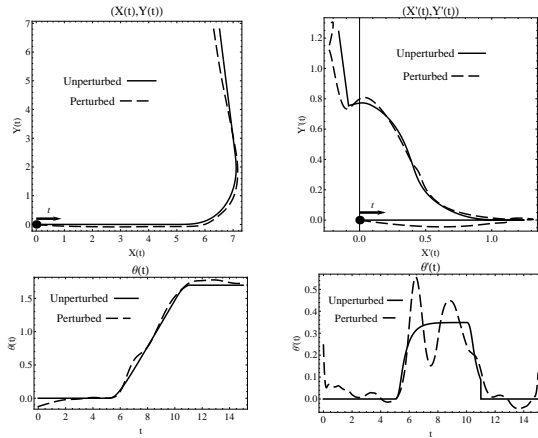


Fig. 5. Comparison of the perturbed $\bar{h}(t)$ with the unperturbed $h(t)$.

With a set of perturbed measured trajectories, the optimization techniques may now be applied to find the mode sequence and optimal switching times that correspond to $\bar{h}(t)$. Using the same cost function, with the same Q , R and P as in Example 2, we first conduct the relaxed switched system optimization. The resulting optimal relaxed control input, $\hat{u}^*(t)$, is in Fig 6. These control inputs correspond to a mode sequence of $\Psi = (1, 4, 2, 4, 1)$ and switching times $\mathcal{T} = (5.0987, 8.0416, 8.7065, 11.4723)^T$.

The sub-system $\sigma = 2$ exists for only 0.6649s. Furthermore, it is only slightly the most active sub-system for its short time period. An obvious option is to implement a heuristic with the purpose of removing modes from the mode sequence that exhibit similar behavior to $\sigma = 2$. This line of reasoning is also presented in [7]. If $\sigma = 2$ were removed, the mode estimation routine would correctly estimate the desired mode sequence, Ψ^d .

In order to demonstrate that the mode estimation may be used in conjunction with a switching time optimization routine, we use the estimated pair, (\mathcal{T}, Ψ) , as initial parameters. Algorithms for switching time optimization using the first-

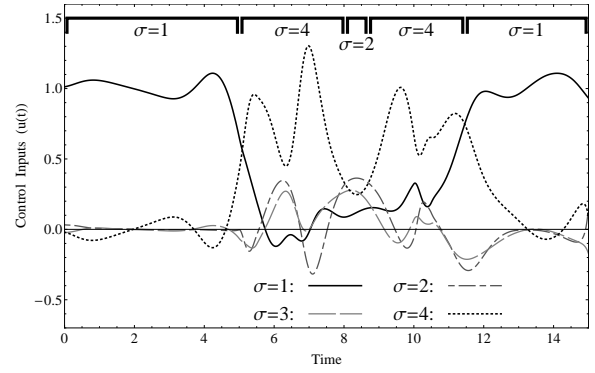


Fig. 6. Plot of the optimal relaxed control inputs for Example 2. Each control input corresponds to a sub-system σ . The sequence of greatest control inputs corresponds to a mode sequence of $\Psi = (1, 4, 2, 4, 1)$. These modes transition at times $\mathcal{T} = (5.0987, 8.0416, 8.7065, 11.4723)^T$

order descent direction are in [4], [6], [7], [21]. We choose a cost function

$$J(\mathcal{T}, \Psi) = \int_{T_0}^{T_N} \frac{1}{2} (x(\tau) - h(\tau))^T Q (x(\tau) - h(\tau)) d\tau + \frac{1}{2} (x(T_N) - h(T_N))^T P (x(T_N) - h(T_N))$$

where $Q = \text{diag}(1, 1, 1, 1, 1, 1)$ and $P = \text{diag}(1, 10, 1, 10, 1, 1)$. Switching time optimization shall now be conducted. After the second step of descent, the $\sigma = 2$ sub-system exists for less than 0.1 seconds, so we remove it, leaving $\Psi = (1, 4, 1)$. With this removal, the switching time optimization converges to optimal solution $\mathcal{T}^* = (4.8537, 10.9376)^T$. These optimal switching times are approximately $\mathcal{T}^d = (5, 11)^T$ despite the large variance of friction, the slow sample rate of the GPS and the GPS sensor error. Fig 7 compares the X-Y trajectories computed using the optimal switching times with the measured trajectories $\bar{h}(t)$ as well as showing the performance metric $\ell(x(t))$ for the optimized system.

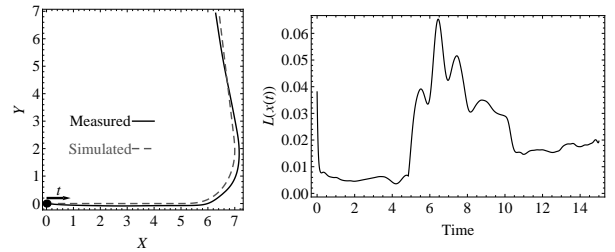


Fig. 7. (left) X-Y plot of the simulated trajectories corresponding to the optimal switching times compared with the measured trajectories $h(t)$ and (right) plot of the performance metric $\ell(x(t))$.

V. CONCLUSION

This paper models the interaction of the SSV’s wheels with the ground as Coulomb friction in order to partition the SSV into a switched system. Doing this simplifies the

representation of maneuvers of the SSV to the pair (\mathcal{T}, Ψ) , where the switching times, \mathcal{T} , are the times at which the modes from the mode sequence Ψ transition.

The switching times are estimated using switching time optimization (see [4], [6], [7], [21]). This optimization assumes a mode sequence. This paper removes the assumption by presenting an approach for estimating a mode sequence. The approach optimizes a relaxed infinite dimensional representation of switched systems and projects the optimal solution back onto the set of feasible solutions. Examples demonstrate that the presented mode estimation approach performs well despite model and sensor disturbances.

REFERENCES

- [1] Georgia Anousaki and K. J. Kyriakopoulos. A dead-reckoning scheme for skid-steered vehicles in outdoor environments. *International Conference on Robotics and Automation*, 1:580–585, 2004.
- [2] Georgia C. Anousaki and Konstaninos J. Kyriakopoulos. Simultaneous localization and map building of skid-steered robots. *IEEE Robotics and Automation Magazine*, pages 79–89, 2007.
- [3] Yoav Benjamini and Yosef Hochberg. Controlling the false discovery rate: a practical and powerful approach to multiple testing. *Journal of the Royal Statistical Society*, 1995.
- [4] T. M. Caldwell and T. D. Murphey. Second-order optimal estimation of slip state for a simple slip-steered vehicle. *IEEE Conference on Automation Science and Engineering*, Fix:Fix, 2009.
- [5] Luca Caracciolo, Alessandro De Luca, and Stefano Iannitti. Trajectory tracking control of a four-wheel differentially driven mobile robot. *International Conference on Robotics and Automation*, 4:2632–2638, 1999.
- [6] Florent C. Delmotte. *Multi-Modal Control: From Motion Description Languages to Optimal Control*. PhD thesis, Georgia Institute of Technology, 2006.
- [7] M. Egerstedt, Y. Wardi, and F. Delmotte. Optimal control of switching times in switched dynamical systems. *IEEE Conference on Decision and Control*, 3:2138–2143, 2003.
- [8] Magnus Egerstedt, Shun ichi Azuma, and Yorai Wardi. Optimal timing control of switched linear systems based on partial information. *Nonlinear Analysis: Theory, Methods and Applications*, 65:1736–1750, 2006.
- [9] John Hauser. A projection operator approach to the optimization of trajectory functionals. *IFAC World Congress*, 2002.
- [10] John Hauser and David G. Meyer. The trajectory manifold of a nonlinear control system. *IEEE Conference on Decision and Control*, 1:1034–1039, 1998.
- [11] Sture Holm. A simple sequentially rejective multiple test procedure. *Scand J Statist*, pages 65–70, 1979.
- [12] Krzysztof Kozłowski and Dariusz Pazderski. Modeling and control of a 4-wheel skid-steering mobile robot. *Int. J. Appl. Math. Comput. Sci.*, pages 477–496, 2004.
- [13] Todd D. Murphey. Kinematic reductions for uncertain mechanical contact. *Robotica*, 25:751–764, 2007.
- [14] R.M. Murray, Z. Li, and S.S. Sastry. *A Mathematical Introduction to Robotic Manipulation*. CRC Press, 1994.
- [15] Axel Schild, Xu Chu Ding, Magnus Egerstedt, and Jan Lunze. Design of optimal switching surfaces for switched autonomous systems. *IEEE Conference on Decision and Control*, 2009. (submitted).
- [16] Zibin Song, Yahya H Zweiri, and Lakmal D Seneviratne. Non-linear observer for slip estimation of skid-steering vehicles. *International Conference on Robotics and Automation*, pages 1499–1504, 2006.
- [17] John D. Storey and Robert Tibshirani. Statistical significance for genomewide studies. *PNAS*, 2003.
- [18] T. H. Tran, N. M. Kwok, S. Scheding, and Q. P. Ha. Dynamic modelling of wheel-terrain interaction of a UGV. *IEEE Conference on Automation Science and Engineering*, pages 369–374, 2007.
- [19] Erik I. Verriest. Optimal control for switched point delay systems with refractory period. *IFAC World Congress*, 2005.
- [20] Y. Wardi, X.C. Ding, M. Egerstedt, and S. Azuma. On-line optimization of switched-mode systems: Algorithms and convergence properties. *IEEE Conference on Decision and Control*, 46, 2007.
- [21] Xuping Xu and Panos J. Antsaklis. Optimal control of switched autonomous systems. *IEEE Conference on Decision and Control*, 41:4401 – 4406, 2002.
- [22] Jingang Yi, Dezhen Song, Junjie Zhang, and Zane Goodwin. Adaptive trajectory tracking control of skid-steered mobile robots. *IEEE Conference on Robotics and Automation*, pages 2605–2610, 2007.